

Finite Element Modeling of Small- and Medium-Sized Full Thickness Rotator Cuff Tears

Mason J. Garcia^{1,2}, Gabriel Landi¹, Bailee Covan¹, Daniela Caro¹, Arun J. Ramappa^{1,3}, Joseph P. Deangelis^{1,3}, Ara Nazarian^{1,2,3}
¹ Musculoskeletal Translational Innovation Initiative, Beth Israel Deaconess Medical Center, Harvard Medical School, Boston, MA, USA
² Boston University, Mechanical Engineering Department, Boston, MA, USA
³ Carl J. Shapiro Department of Orthopaedic Surgery, Beth Israel Deaconess Medical Center, Harvard Medical School, Boston
Mgarci15@bidmc.harvard.edu

Disclosures: The authors do not have any disclosures.

Introduction: Shoulder pain is the third most common musculoskeletal complaint reported to general practitioners in primary care settings. Of shoulder injuries, rotator cuff (RC) tears are among the most prevalent, as they are present in 23% of the population. Although they are frequently asymptomatic, 36% progress into symptomatic tears. Due to the structural and mechanical inhomogeneity of the supraspinatus tendon, rotator cuff tear pathology is poorly understood, making it difficult to manage clinically. Finite element (FE) modeling is a useful tool to evaluate the mechanical environment of the supraspinatus tendon, which cannot be measured *in vivo*; however, their clinical utility largely depends on the ability to predict tissue deformation accurately. Tendons exhibit a hyper-elastic material response due to the recruitment and alignment of collagen fibers. The aim of this study is to evaluate the internal strains for small- and medium-sized RC tears under daily living and exercise rehabilitation loads to assess the risk for potential tear progression.

Methods: Six fresh-frozen intact human shoulders (Medcure, Inc, Providence, RI) with a mean age of 65 ± 9 were used after verifying no sign of RCT, fraying, or delamination of the rotator cuff tendons. The skin and the muscles, excluding the supraspinatus, infraspinatus, and subscapularis muscles, were removed, and the supraspinatus tendons were then isolated and detached from the humeral head at the insertion site. All tendons were split into thirds to separate the anterior, middle, and posterior regions. These regions were then further split into medial and lateral regions and articular and bursal regions, resulting in 12 samples per tendon that were roughly $5 \times 10 \times 1$ mm. To obtain the mechanical properties (stress-strain curves) for each tendon region, samples were subjected to uniaxial tensile testing (UniVert, CellScale Biomaterials Testing, ON, Canada) to 10% strain to avoid any permanent damage to the samples. After mechanical testing, three $10 \mu\text{m}$ slices were taken every $250 \mu\text{m}$, stained with Masson's trichrome staining, and imaged using a $10\times$ brightfield microscope (Olympus VS120) to quantify the collagen orientation. To characterize the tendon regions to use in an FE model, collagen orientation and the stress-strain curves were used as inputs to fit the Holzapfel-Gasser-Ogden model for soft tissue to determine the appropriate material parameters for FE modeling. Using previously validated supraspinatus-infraspinatus model geometry, crescent-shaped tears were created (Materialise 3-Matic [Leuven Belgium](#)) in the posterior third of the supraspinatus tendon, as this region has recently been thought to be the origin of RC tears to represent small- and medium-sized RC tears (**Table 1**). Based on reported data for maximum voluntary contractile force (MVC) of the supraspinatus and percentage of MVC for daily living and rehabilitation exercises was determined for the supraspinatus and infraspinatus (**Table 2**).

Results: Maximum principal strains on the articular and bursal sides of the tendon were taken at the anterior and posterior edges of the tear tips (**Figure 1**). Generally, as tear size increased, so did strain; however, the increase in strain may not be clinically relevant as the strain was less than the failure strain that causes tear progression. For the case of small tears (20% and 30%), the bursal side experienced more strain at the anterior tip compared to the articular side for both prone abduction ($p=0.03$) and external rotation ($p=0.01$). However, as tear size increased, the articular side had more strain at the anterior tear tip compared to the bursal side for both prone abduction ($p<0.0001$) and external rotation ($p<0.0001$). Previous cadaveric studies have evaluated the maximum principal strain that causes significant tear propagation and found that tears will progress at 26.1 ± 9.4 % of strain. Using 26.1% strain as failure criteria (**Figure 2**), we observed that for prone abduction, there was a potential risk for tear progression for medium sized tears (40% and 50%). The strain was always lower than 26.1% for all tear sizes for external rotation, suggesting that this rehabilitation exercise may not put patients at risk for tear progression. For all daily activities (typing, drinking, and brushing teeth), the strain never exceeded 16.7%, at the low end of a strain that causes tear progression. This suggests that daily activities are unlikely to cause tear progression.

Discussion: FE modeling provides insight into the internal strains that the RC experiences that cannot be measured *in vivo* which is valuable to understanding which patients may or not be at risk for tear progression. For small- and medium-sized RC tears, physical therapy has a success rate of 75%, with tear progression and continued symptoms being a common cause of failure. However, this could be addressed by understanding the strain the tendon is under during rehabilitation and developing individualized care plans considering tear size and the loads applied to the tendon to avoid the potential for tear progression.

Clinical Relevance: Patient-specific FE modeling is useful clinically to determine the risk of tear progression based on patient-specific material properties and tear characteristics. This study supports the current risk management plans for small RC tears. However, a better understanding of tear characteristics and loads applied in rehabilitation for medium-sized tears are warranted to understand best what exercises may or may not suit patients.

Table 1. Tear Characteristics

| Tear Size | Anterior-Posterior Length (mm) | Medial-Lateral Length (mm) |
|-----------|--------------------------------|----------------------------|
| 20% | 5.6 | 5.6 |
| 30% | 8.4 | 8.4 |
| 40% | 11.2 | 11.2 |
| 50% | 14 | 14 |

Table 2. Loading Conditions for Activities

| Activity | Supraspinatus Load (N) | Infraspinatus Load (N) |
|------------------------------------|------------------------|------------------------|
| Typing | 52 | 86 |
| Drinking | 144 | 124 |
| Brushing Teeth | 83 | 139 |
| Prone Abduction | 392 | 344 |
| External Rotation at 90° Abduction | 563 | 268 |

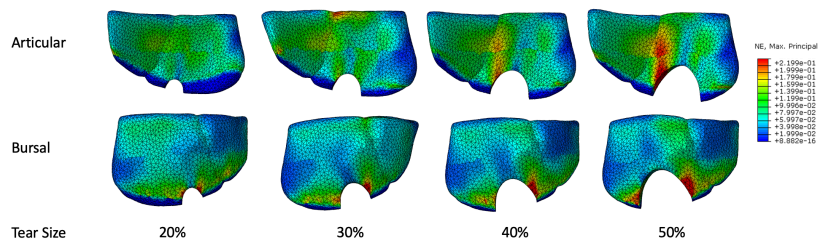


Figure 1. Finite element model maximum principal strains for increasing tear size.

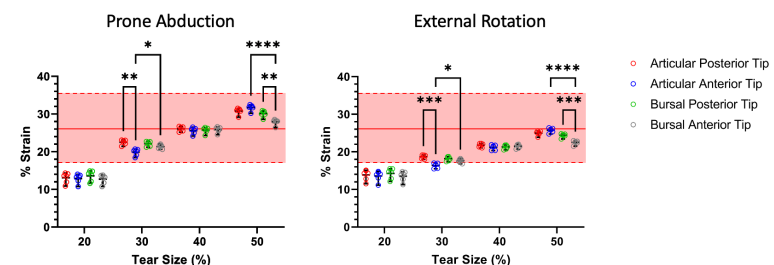


Figure 2. Maximum principal strains at the tear tips. Red box represents the range of tendon strain that results in tear progression from previous cadaveric studies.